

Precipitation–Surface Temperature Relationship in the IPCC CMIP5 Models

WU Renguang^{*1} (吴仁广), CHEN Jiepeng² (陈洁鹏), and WEN Zhiping² (温之平)

¹*Institute of Space and Earth Information Science, The Chinese University of Hong Kong,
Hong Kong*

²*Center for Monsoon and Environment Research/Department of Atmospheric Sciences,
Sun Yat-Sen University, Guangzhou 510275*

(Received 17 June 2012; revised 17 August 2012)

ABSTRACT

Precipitation and surface temperature are two important quantities whose variations are closely related through various physical processes. In the present study, we evaluated the precipitation–surface temperature (P–T) relationship in 17 climate models involved in the Coupled Model Intercomparison Project Phase 5 (CMIP5) for the IPCC Assessment Report version 5. Most models performed reasonably well at simulating the large-scale features of the P–T correlation distribution. Based on the pattern correlation of the P–T correlation distribution, the models performed better in November–December–January–February–March (NDJFM) than in May–June–July–August–September (MJJAS) except for the mid-latitudes of the Northern Hemisphere, and the performance was generally better over the land than over the ocean. Seasonal dependence was more obvious over the land than over the ocean and was more obvious over the mid- and high-latitudes than over the tropics. All of the models appear to have had difficulty capturing the P–T correlation distribution over the mid-latitudes of the Southern Hemisphere in MJJAS. The spatial variability of the P–T correlation in the models was overestimated compared to observations. This overestimation tended to be larger over the land than over the ocean and larger over the mid- and high-latitudes than over the tropics. Based on analyses of selected model ensemble simulations, the spread of the P–T correlation among the ensemble members appears to have been small. While the performance in the P–T correlation provides a general direction for future improvement of climate models, the specific reasons for the discrepancies between models and observations remain to be revealed with detailed and comprehensive evaluations in various aspects.

Key words: precipitation-surface temperature relationship, CMIP5 models, seasonal dependence

Citation: Wu, R. G., J. P. Chen, and Z. P. Wen, 2013: Precipitation–surface temperature relationship in the IPCC CMIP5 Models. *Adv. Atmos. Sci.*, **30**(3), 766–778, doi: 10.1007/s00376-012-2130-8.

1. Introduction

Numerical simulation with climate models is an important approach to understanding climate changes in the history and projections of climate in the future. Climate models are approximations of the real world. Thus, systematic biases in mean states and uncertainty in future projections are inevitable in climate models. For a proper application of climate model simulations, it is necessary to evaluate the performance of climate models in various aspects. Given the availabil-

ity of the new version of climate model simulations aimed at providing the basis for the IPCC's Assessment Report version 5 (AR5) in the coming years, we evaluated the models' performance in climate simulations.

In this study, we evaluated the precipitation–surface temperature (P–T) relationship. There are several reasons for choosing this topic. First, precipitation and surface temperature are two important quantities in climate studies that are directly related to our lives. Second, the variations in these two variables are

^{*}Corresponding author: WU Renguang, renguang@cuhk.edu.hk

closely related in different ways that indicate different physical connections between them. A positive P–T correlation indicates an oceanic forcing of precipitation in which higher SST and more precipitation follow the ocean surface warming (Wu et al., 2006). In contrast, more precipitation reduces downward shortwave radiation reaching the earth's surface and thus leads to surface cooling, which contributes to a negative P–T correlation (Trenberth and Shea, 2005). Surface latent heat flux anomalies associated with precipitation and wind changes can influence SST and thus modulate the P–T correlation (e.g., Wu and Kirtman, 2007; Wu et al., 2009). Thus, the performance of the climate models in the P–T relationship provides information about whether the physical processes in the models are realistic, which contributes to understanding the biases that may appear in precipitation and surface temperature variations. Third, the P–T relationship has not been evaluated systematically over the global domain according to the literature. Previous evaluations have been limited to several individual models (e.g., Trenberth and Shea, 2005; Wu et al., 2006).

Pronounced seasonal change and regional feature has been identified in the P–T relationship. A positive P–T correlation has been observed in the equatorial central-eastern Pacific Ocean through the year (Trenberth and Shea, 2005; Wu et al., 2006; Wu and Kirtman, 2007). In contrast, the P–T correlation in the tropical western Pacific warm pool and Indonesian regions depends on the season: positive in boreal winter and negative in boreal summer (Wu and Kirtman, 2007). This seasonality indicates a seasonal change in the ocean-atmosphere connection. A negative P–T correlation prevails over the continental land in summer, whereas a positive P–T correlation is observed in high-latitude land regions in winter (Trenberth and Shea, 2005). The contrast of the P–T correlation between winter and summer over land regions has been pointed out in previous studies in different regions, such as the United States and Canada (Madden and Williams, 1978; Idso and Balling, 1992; Isaac and Stuart, 1992; Zhao and Khalil, 1993), South America (Rusticucci and Penalba, 2000), England and Wales (Tout, 1987), and Switzerland (Rebetez, 1996). The contrast of the P–T relationship between land and ocean regions in the tropics has been noted by Wang et al. (2008). An out-of-phase relationship between decadal precipitation and surface temperature variations has been identified in Australia (Power et al., 1999).

The organization of the text is as follows. The data and methods used in the present study are described in section 2. In section 3, we present the results of the P–T correlation in observations and compare the

model simulations with respect to observations over the global domain, the land, the ocean, the tropics, the mid- and high-latitude regions, respectively. In addition, the spread among model ensemble members is addressed in section 3 as well. A summary is given in section 4.

2. Data and methods

The monthly mean precipitation from version 2 of the Global Precipitation Climatology Project (GPCP) (Adler et al., 2003) was used as a proxy for observations. GPCP precipitation data were available on a $2.5^\circ \times 2.5^\circ$ grid over the global domain from 1979 to 2010. The University of Delaware monthly mean precipitation and surface air temperature data (http://www.cdc.noaa.gov/cdc/data/UDel_AirT_Precip.html) were used in this study. This dataset was produced by combining a large number of stations, both from the Global Historical Climatology Network (GHCN; Vose et al., 1992) and, more extensively, from the archive of Legates and Willmott (Legates and Willmott, 1990). This dataset has a resolution of $0.5^\circ \times 0.5^\circ$ covering the land for the period 1901–2008, provided by the National Oceanic and Atmospheric Administration's Oceanic and Atmospheric Research's Earth System Research Laboratory (NOAA/OAR/ESRL), Physical Sciences Division (PSD), Boulder, Colorado, USA, from its website at <http://www.esrl.noaa.gov/psd/>. Over the oceans, we used the SST data from the NOAA Extended Reconstruction SST, version 3 (Smith et al., 2008), which was provided by NOAA/OAR/ESRL PSD, Boulder, Colorado, USA, from its website at <http://www.cdc.noaa.gov/>. This SST dataset has a resolution of $2.0^\circ \times 2.0^\circ$ and covers 1854 to the present.

Monthly mean precipitation, surface air temperature, and surface skin temperature from 17 models of the IPCC Coupled Model Intercomparison Project phase 5 (CMIP5; Taylor et al., 2012) were used in this study (Table 1). The model outputs used in the present analysis were obtained from historical simulations. The IPCC CMIP5 provided a large amount of model outputs that require a substantial time to download through the Internet. Here, we only analyzed one member for each of the 17 models for a fair comparison with one realization of observations. For some selected models with multiple simulations, we analyzed all of the simulations to address the spread of the results among the model members.

The IPCC CMIP5 models have different spatial resolutions. For a fair comparison with observations, we interpolated the precipitation and surface temperature to a common $2^\circ \times 2^\circ$ grid for both the obser-

Table 1. Information of the 17 climate models used in the present analysis.

Institute	Model	Resolution Grid numbers: lon*lat
BCC	BCC-CSM1.1	128×64
BNU	BNU-ESM	128×64
CCCMA	CanCM4	128×64
NCAR	CCSM4	288×192
CNRM-CERFACS	CNRM-CM5	256×128
CSIRO-QCCCE	CSIRO-Mk3.6.0	192×96
LASG-IAP	FGOALS-S2.0	128×108
NOAA-GFDL	GFDL-CM3	144×90
NASA-GISS	GISS-E2-R	144×90
NIMR-KMA	HadGEM2-AO	192×145
MOHC	HadGEM2-CC	192×145
INM	INM-CM4	180×120
IPSL	IPSL-CM5A-LR	96×96
MIROC	MIROC4h	640×320
MPI-M	MPI-ESM-P	192×96
MRI	MRI-CGCM3	320×160
NCC	NorESM1-ME	144×96

Institute Acronyms

BCC: Beijing Climate Center, China Meteorological Administration

BNU: College of Global Change and Earth System Science, Beijing Normal University

CCCMA: Canadian Centre for Climate Modeling and Analysis

NCAR: National Center for Atmospheric Research

CNRM-CERFACS: Centre National de Recherches Meteorologiques/Centre Europeen de Recherche et Formation Avancees en Calcul Scientifique

CSIRO-QCCCE: Commonwealth Scientific and Industrial Research Organization in collaboration with Queensland Climate Change Centre of Excellence

LASG-IAP: LASG, Institute of Atmospheric Physics, Chinese Academy of Sciences

NOAA-GFDL: NOAA Geophysical Fluid Dynamics Laboratory

NASA-GISS: NASA Goddard Institute for Space Studies

NIMR-KMA: National Institute of Meteorological Research/Korea Meteorological Administration

MOHC: Met Office Hadley Centre

INM: Institute for Numerical Mathematics

IPSL: Institut Pierre-Simon Laplace

MIROC: Atmosphere and Ocean Research Institute (The University of Tokyo), National Institute for Environmental Studies, and Japan Agency for Marine-Earth Science and Technology

MPI-M: Max Planck Institute for Meteorology

MRI: Meteorological Research Institute

NCC: Norwegian Climate Centre

vations and the model simulations. To examine the dependence of the results on the spatial resolution, we performed a parallel analysis of the correlation for precipitation and surface temperature interpolated to a $0.5^\circ \times 0.5^\circ$ grid. The results were very similar. In this report, we only show maps for correlations calculated on the $2^\circ \times 2^\circ$ grid.

The historical simulations of the IPCC models covered more than 100 years up to 2005. The GPCP precipitation was only available from 1979. In this analysis, the P–T correlation was calculated for a common period 1979–2005 in both observations and models. This parameter was chosen for convenience of comparison of the magnitude of the correlation between

the observations and model simulations because the significance of the correlation depends on the number of years used in the correlation calculation.

The P–T correlation changes with season (Trenberth and Shea, 2005; Wu and Kirtman, 2007). Thus, it was necessary to calculate the correlation for different seasons to understand the seasonal dependence of the relationship and the model performance. Following Trenberth and Shea (2005), the P–T correlation was calculated for groups of months for both observations and model simulations: May–June–July–August–September (MJJAS) and November–December–January–February–March (NDJFM).

The P–T correlation is a two-dimensional field that

includes both the pattern and magnitude of the correlation. In this study, we used the Taylor diagram (Taylor, 2001) to quantify the model performance in simulating the P–T correlation field. Only a short description is given here. The Taylor diagram provides information about the pattern correlation, the ratio of the standard deviation, and the root-mean-square difference of the P–T correlation between model simulations and observations. The diagram only displays two quantities (the pattern correlation and the ratio of the standard deviation), with the third quantity related to the first two quantities through the Law of Cosine. On the Taylor diagram, the observed field (the P–T correlation in this study) is represented by one point (the reference point) with unit correlation coefficient and unit standard deviation, which is on the abscissa. The model points are plotted based on the pattern correlation and the ratio of the standard deviation with respect to the observations. The distance of the model points from the reference point is determined by both the pattern correlation and the ratio of the standard deviation. The closer the model point to the reference point, the shorter the distance, a better agreement between the model simulation and observation in the P–T correlation. Visually, the Taylor diagram shows the relative contribution of the pattern correlation and the variance to the good or bad performance of a model.

3. Results

3.1 Observations

Figure 1 shows the distribution of the P–T correlation calculated for groups of months: MJJAS and NDJFM. According to the availability of observations, the correlation over land was based on the University of Delaware precipitation and surface air temperature data; the data over the ocean was based on GPCP precipitation and Extended Reconstruction of Sea Surface Temperature version 3 (ERSST v3) SST. The distribution of the P–T correlation displays obvious regional features and seasonal dependence (Fig. 1).

In MJJAS, there is a large and positive P–T correlation over the equatorial central-eastern Pacific Ocean (Fig. 1a). A positive correlation was also seen over the equatorial Atlantic Ocean, the western and eastern equatorial Indian Ocean, and the Antarctic region. A negative P–T correlation dominates over the Northern Hemisphere land regions as well as over equatorial South America and the Indonesian land regions. The largest negative correlation appeared over southeastern Europe, eastern China, India, the western United States, and western tropical North Africa. A weak negative correlation was obtained over the mid-latitudes of the North Pacific and North Atlantic regions.

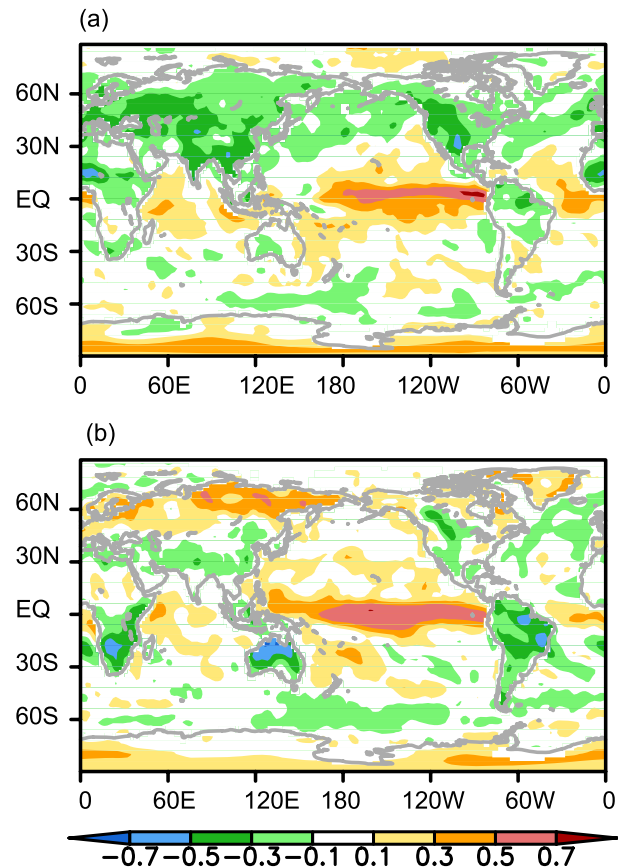


Fig. 1. Point-wise correlation between observed monthly mean anomalies of precipitation and surface temperature (surface air temperature over the land and SST over the ocean) for groups of months of (a) MJJAS and (b) NDJFM during 1979–2005.

In NDJFM, a large positive correlation extended from the equatorial eastern Pacific to the equatorial western Pacific (Fig. 1b). There was a positive correlation over the equatorial Atlantic Ocean and the equatorial western Indian Ocean, the South Pole region, and the high-latitude land regions of the Northern Hemisphere. Negative correlation was obtained over the Southern Hemisphere land regions as well as over the Rocky Mountain region and the subtropical Asian region.

The P–T correlation over the continental regions exhibited obvious differences between MJJAS and NDJFM. The negative P–T correlation was large in the summer hemispheres but weak in winter hemispheres. In the Northern Hemisphere high-latitudes, the P–T correlation switched from weakly negative to strongly positive over northern Eurasia, northeast Canada, and Greenland. In the Antarctic region, the positive correlation enhances from summer to winter. The most noticeable seasonal change over the ocean occurred in

the equatorial eastern Indian Ocean and the tropical western North Pacific. In the former region, the P–T correlation was large and positive in boreal summer but weak in boreal winter. In the latter region, the P–T correlation was positive in boreal winter and weak negative in boreal summer. There was a noticeable seasonal change in the mid-latitude North Pacific, where the correlation was negative in MJJAS but weak in NDJFM. The negative P–T correlation in MJJAS is likely related to the impact of precipitation on SST through cloud and radiation changes along the storm track (Wu and Kinter, 2010). This cloud-radiation effect was weak in boreal winter.

The P–T correlation in the present study was generally consistent with previous studies. The prevalence of the positive correlation over most of the equatorial oceanic regions, the seasonal change over the continents with negative correlation in summer hemispheres, and the positive correlation over the high-latitude lands of the Northern Hemisphere in winter agreed well with Trenberth and Shea (2005). The seasonal changes in different land regions were consistent with previous regional studies (Madden and Williams, 1978; Tout, 1987; Isaac and Stuart, 1992; Zhao and Khalil, 1993; Rusticucci and Penalba, 2000). The seasonal changes observed over the equatorial eastern Indian Ocean and the tropical western North Pacific were consistent with Trenberth and Shea (2005) and Wu and Kirtman (2007).

There were, however, several notable discrepancies between the present study and Trenberth and Shea (2005). The positive P–T correlation over the equatorial western Pacific in NDJFM appeared larger than that obtained by Trenberth and Shea (2005). Trenberth and Shea (2005) obtained a positive correlation along the Antarctic coast, which was not seen in this study. A positive correlation appeared over the mid-latitude oceans of the Southern Hemisphere in MJJAS in Trenberth and Shea (2005), but not in this study. The negative correlation over the tropical western North Pacific in summer appeared smaller than in Trenberth and Shea (2005). In this study a large positive correlation was obtained in the South Pole region where Trenberth and Shea (2005) got a negative correlation. These discrepancies occurred due to the differences in the datasets. Trenberth and Shea (2005) used the European Center for Medium-range Weather Forecasts 40-year reanalysis (ERA40) surface air temperature and GPCP precipitation. We examined the local correlation of the ERA40 surface air temperature with the University of Delaware surface air temperature over the land and the ERSST3 SST over the ocean as well as the local correlation of the GPCP precipitation with the University of Delaware precipitation over

the land. Relatively low correlation (correlation coefficient <0.6) between the ERA40 surface air temperature and ERSST3 SST was obtained over the tropical western North Pacific and middle and high latitudes of the Southern Hemisphere. This appears to be the reason for the discrepancies in the tropical western Pacific and along the coast of Antarctic continent. The correlation between the GPCP precipitation and the University Delaware precipitation was low (<0.4) over the Antarctic continent, which likely contributed to the discrepancy there.

As pointed out by Trenberth and Shea (2005), the regional and seasonal changes in the P–T correlation indicate different connections between precipitation and surface temperature variations. The positive correlation over the equatorial oceans indicates the oceanic forcing of precipitation (Wu et al., 2006; Wu and Kirtman, 2007). The equatorial Pacific warming during El Niño events induced anomalous heating and more precipitation (Wu et al., 2006). Similar forcing was observed in the equatorial Atlantic and the equatorial Indian Ocean (Wu and Kirtman, 2007), though it was not as prevalent as in the equatorial Pacific. Over the continental land regions, the negative correlation appeared because of the surface temperature decrease following the suppression of downward solar radiation associated with the precipitation increase (Trenberth and Shea, 2005). This type of physical connection can also be seen over the tropical western North Pacific in summer (Wu and Kirtman, 2007). The positive correlation over the high-latitude land regions in winter occurred because the atmosphere cannot hold much moisture when the temperature is very low, and thus little precipitation occurs. The north–south contrast of correlation over Europe in winter is related to the shift of the North Atlantic storm track. A northward (southward) shift of the storm track would bring warmer (colder) and wetter (drier) air to northern Europe, resulting in a positive P–T correlation, whereas the southern Europe would experience drier (wetter) condition, leading to a negative P–T correlation (Trenberth and Shea, 2005).

3.2 Model simulations

Figure 2 shows the Taylor diagram indicating the P–T correlation in the 17 climate model simulations compared to the observations over the global domain for groups of months of MJJAS and NDJFM, respectively. The P–T correlation was calculated based on precipitation and surface air temperature over the land regions and based on precipitation and surface skin temperature over the oceanic regions. Each point corresponded to a single simulation of a specific model (Fig. 2). The radial distance of the points from the

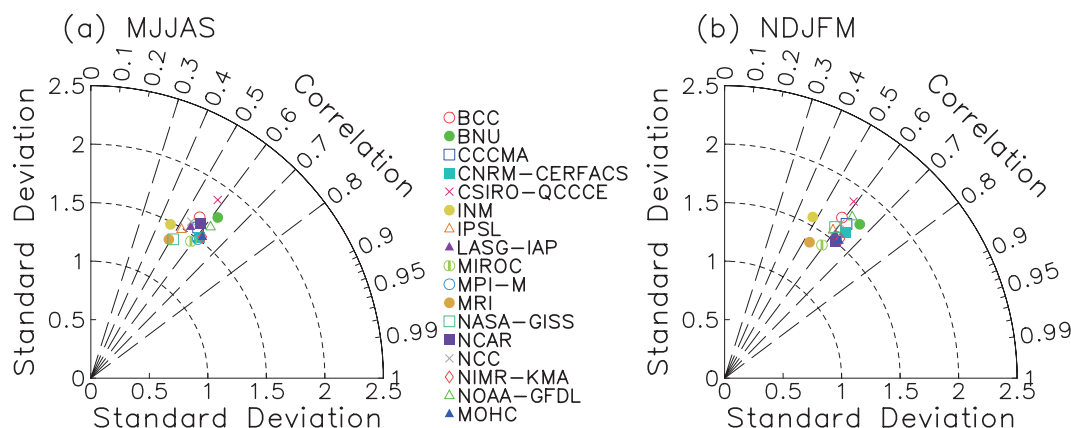


Fig. 2. The Taylor diagram showing the pattern statistics of the P–T correlation on $2^\circ \times 2^\circ$ grids over the global domain for 17 climate model simulations compared to the observations for groups of months of MJJAS (a) and NDJFM (b) during 1979–2005.

origin was the ratio of the standard deviation of the model simulated P–T correlation field with respect to the standard deviation of the observed P–T correlation field. We noted that the standard deviation indicated the spatial variability of the P–T correlation. The azimuthal location of the points indicated the pattern correlation coefficient between the simulated and observed P–T correlation fields. The observation point (the reference point for comparison with model simulations) was on the abscissa, with one unit of standard deviation. In calculating the pattern correlation and the standard deviation for the Taylor diagram, the P–T correlation was multiplied by the cosine of the latitude to take into account of the decrease of the longitude–latitude grid-cell area with the latitude.

Most of the points derived from the 17 climate model simulations tended to be close to each other (Fig. 2). This indicates general agreement among models in simulating the P–T correlation over the global domain. In MJJAS, most of the points had a pattern of correlation of 0.50–0.62 and a standard deviation of

1.3–1.7 (Fig. 2a). In NDJFM, most of the points had a pattern correlation of 0.58–0.64 and a standard deviation of 1.5–1.8 (Fig. 2b). In comparison, the model simulations agreed with the observations better in NDJFM than in MJJAS based on the pattern correlation. In both MJJAS and NDJFM, the P–T correlation showed larger spatial variability in models than in observations by $\sim 50\%$ – 60% . The CSIRO model exhibited the largest standard deviation, whereas the MRI exhibited the smallest standard deviation in both MJJAS and NDJFM. The BNU model had the largest pattern correlation in NDJFM. The INM model had the lowest pattern correlation in both MJJAS and NDJFM. The MRI model had a pattern correlation second to the INM.

The P–T correlation differed over the ocean and the land regions (Fig. 1). In particular, the correlation over continental land regions displayed a large seasonal change. To examine the model performance in the P–T correlation over the land and ocean regions separately, the Taylor diagrams constructed based on the

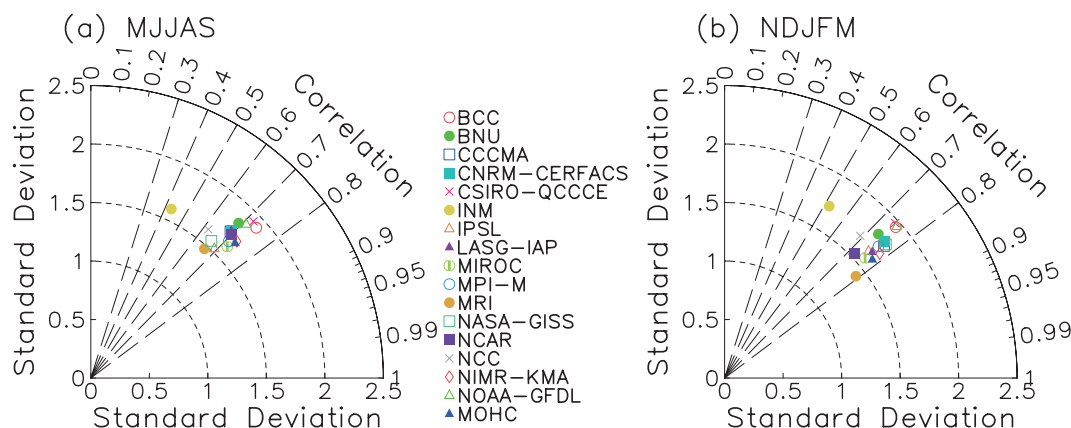


Fig. 3. The same as Fig. 2 except for the land.

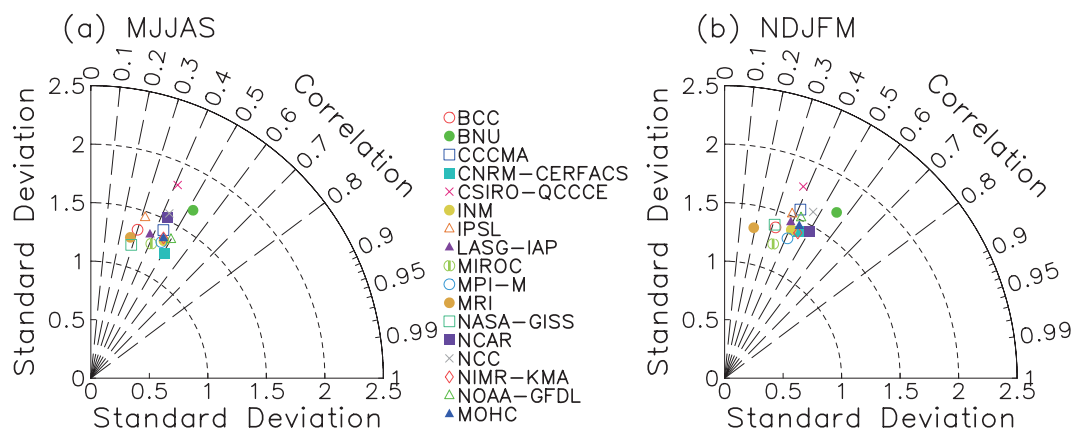


Fig. 4. The same as Fig. 2 except for the ocean.

land and oceanic grids, respectively, for the 17 model simulations (Figs. 3 and 4).

Over land, the pattern correlation was ~ 0.7 , and the standard deviation varied from 1.5 to 2.0 in MJJAS (Fig. 3a). In NDJFM, the pattern correlation was ~ 0.75 (Fig. 3b), higher than in MJJAS. The INM model deviated greatly from the other models, with the pattern correlation of 0.42 in MJJAS and 0.52 in NDJFM, respectively. Like the global domain, the CSIRO model showed the largest standard deviation and the MRI model showed the smallest standard deviation in both MJJAS and NDJFM. One notable feature was that the pattern correlation tended to be larger when the standard deviation was higher in MJJAS. The reason for this may be the following: The magnitude of the P–T correlation indicated the signal for co-variability of precipitation and surface temperature. A higher standard deviation suggests a larger signal for co-variability. The models with a larger signal are expected to capture the P–T correlation distribution better compared to those with a smaller signal.

Over the ocean, the pattern correlation varied from 0.3 to 0.5 in both MJJAS (Fig. 4a) and NDJFM (Fig. 4b). The standard deviation varied from 1.2 to 1.6 in MJJAS and from 1.3 to 1.7 in NDJFM. The CSIRO model showed the largest standard deviation in both MJJAS and NDJFM. The BNU model performed the best and the MRI model was the worst in both MJJAS and NDJFM based on the pattern correlation (Fig. 4b). The BNU model had a large standard deviation, second to the CSIRO model, in both MJJAS and NDJFM. Compared to the land, the pattern correlation was smaller and displayed a larger spread among the models, and the spatial variability of the correlation was smaller. The seasonal dependence of the model performance was not as obvious as over the land. Similar to the land in MJJAS, there was a tendency toward a larger pattern correlation that corre-

sponded to a higher standard deviation in both MJJAS and NDJFM.

The land and ocean coverage varied with the latitude and differed between the Northern and Southern Hemispheres. To examine the impact of the land and ocean distribution, we further evaluated model performance by separating the global domain into the tropics (30°S – 30°N), mid-latitudes (30° – 60°N , 30° – 60°S), and high latitudes (60° – 90°N , 60° – 90°S). The corresponding Taylor diagrams are shown in Fig. 5 (tropics), Fig. 6 (mid-latitudes), and Fig. 7 (high-latitudes).

In the tropics, there was a notable spread among the models (Fig. 5). In MJJAS, the pattern correlation varied from 0.42 to 0.72 and the standard deviation changed from 1.0 to 1.7 (Fig. 5a). In NDJFM, the pattern correlation was mostly between 0.58 and 0.74, and the standard deviation varied from 0.8 to 1.5 (Fig. 5b). The INM model deviated from the other models in NDJFM, with a relatively low pattern correlation. The BNU model had a somewhat higher pattern correlation than the other models in both MJJAS and NDJFM. The IPSL model had the lowest pattern correlation in MJJAS (Fig. 5a). The MRI model displayed the smallest standard deviation in both MJJAS and NDJFM. In comparison, most models performed better in NDJFM than in MJJAS. A tendency for a larger correlation corresponding to a higher standard deviation occurred in both MJJAS and NDJFM.

In the mid-latitudes of the Northern Hemisphere, where land covers a large part, the pattern correlation was mostly between 0.7 and 0.8, and the standard deviation is between 1.0 and 1.5 in MJJAS (Fig. 6a). In NDJFM, most of the models had a pattern correlation between 0.4 and 0.5, and the standard deviation varied from 1.2 to 1.7 (Fig. 6b). The INM model had the lowest pattern correlation in NDJFM and was one of the two models with the lowest pattern correlation in MJJAS, whereas the National Center for Atmospheric

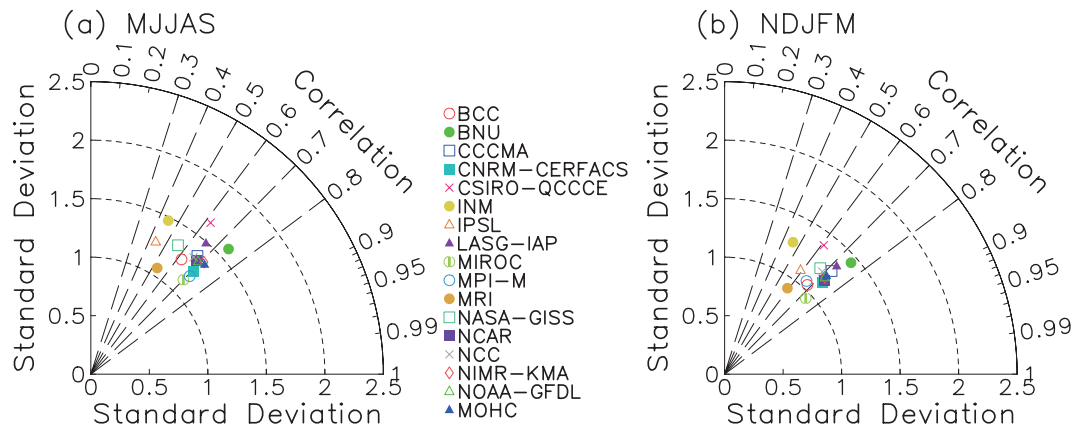


Fig. 5. The same as Fig. 2 except for the tropics (30°S-30°N).

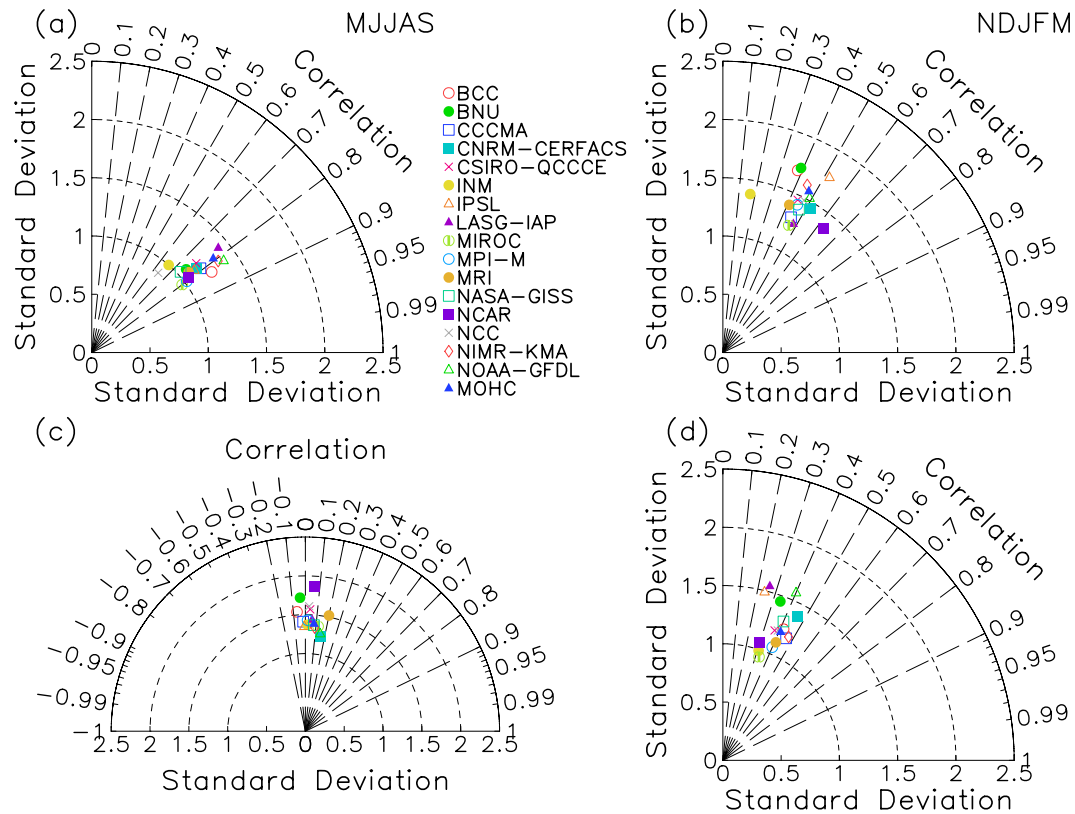


Fig. 6. The same as Fig. 2 except for the mid-latitudes of the Northern Hemisphere (30°-60°N) (a and b) and the mid-latitudes of the Southern Hemisphere (30°-60°S) (c and d).

Research (NCAR) model had the highest pattern correlation in NDJFM. In comparison, the models performed much better in MJJAS than in NDJFM. In the mid-latitudes of the Southern Hemisphere, which is mainly covered by the ocean, the models had difficulty capturing the spatial distribution of the P-T correlation and the standard deviation was ~50% larger than in observations in MJJAS (Fig. 6c). In NDJFM, the pattern correlation varied from 0.3 to 0.5, and the

standard deviation was mostly between 1.0 and 1.5 (Fig. 6d). Thus, the models performed better in NDJFM than in MJJAS, which contrasted sharply with the Northern Hemisphere. In comparison, the model performance was better in the Northern Hemisphere than in the Southern Hemisphere, in summer (Figs. 6a, d) or in winter (Figs. 6b, c).

In the high latitudes of the Northern Hemisphere, the models exhibited a notable spread in MJJAS, with

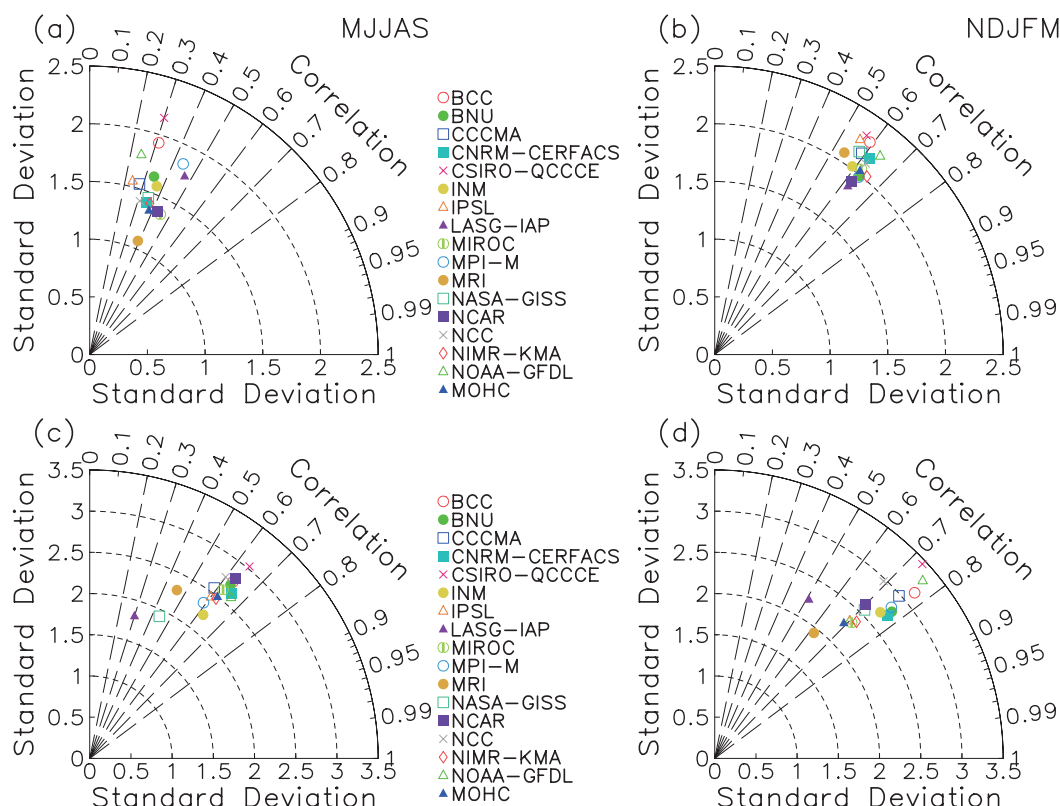


Fig. 7. (a, b) The same as Fig. 2 except for the high-latitudes of the Northern Hemisphere (60° – 90° N) and (c, d) the high-latitudes of the Southern Hemisphere (60° – 90° S).

the pattern correlation varying from 0.2 to 0.5 and the standard deviation varying from 1.4 to 2.0 (Fig. 7a). The CSIRO model had the largest standard deviation, and the MRI model had the lowest standard deviation. In NDJFM, the models were clustered around a pattern correlation of 0.6, and the standard deviation varied between 1.8 and 2.3 (Fig. 7b). In comparison, the models performed much better in NDJFM than in MJJAS based on the pattern correlation. In the high latitudes of the Southern Hemisphere, most of the models had a pattern correlation ~ 0.6 or higher in MJJAS (Fig. 7c). Three models (i.e., LASG-IAP, NASA-GISS, MRI), however, displayed a relatively low pattern correlation. The standard deviation revealed a large spread among the models. In NDJFM, the pattern correlation was mostly ~ 0.7 or greater, except for the LASG-IAP and MRI models (Fig. 7d). The standard deviation varied from 2.0 to 3.5. In comparison, the models captured the distribution of the P–T correlation better in NDJFM than in MJJAS. There was a tendency for a larger pattern correlation to correspond to a higher standard deviation in both MJJAS and NDJFM. In NDJFM, the models displayed a much higher pattern correlation in the Southern Hemisphere than in the Northern Hemisphere (Figs. 7b and d).

From the above comparison, the seasonal dependence was more obvious in the middle and high latitudes than in the tropics. Except for the mid-latitudes of the Northern Hemisphere, the pattern correlation was generally higher in NDJFM than in MJJAS. The land and ocean coverage was an important factor in the performance of the models, which may explain the high pattern correlation in the mid-latitudes of the Northern Hemisphere and the high-latitudes of the Southern Hemisphere as well as the contrast of the pattern correlation between the Northern Hemisphere and the Southern Hemisphere in the summer or winter season. The spatial variability of the correlation tended to increase from lower latitudes to higher latitudes. Another notable feature was that an increase in the pattern correlation tended to accompany an increase in the standard deviation in the tropics and high-latitudes of the Southern Hemisphere.

As noted above, the INM model displayed relatively low pattern correlation compared to the other models over the land, and the MRI model showed a relatively low pattern correlation over the ocean. Therefore, we examined in detail the distribution of the P–T correlation in these two models to understand their performance. For this purpose, we analyzed the dis-

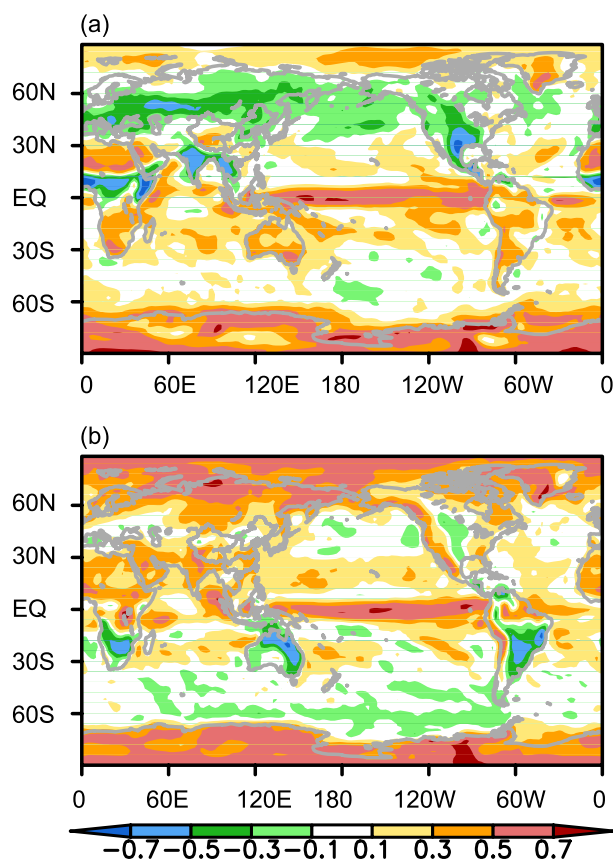


Fig. 8. The same as Fig. 1 except for a single simulation of the INM model.

tribution of the P–T correlation for the INM and MRI models, respectively (Figs. 8 and 9). As in Fig. 1, the correlation was calculated for two groups of months (MJJAS and NDJFM) separately.

For the INM model, most differences from observations occurred over land regions. In MJJAS, large differences from observations occurred over the equatorial western Pacific and the land regions of the Southern Hemisphere, including Australia, southern Africa, and South America (Fig. 8a). In these regions, the observed P–T correlation was weak, whereas the INM model displayed a large positive correlation. Over equatorial South America and western and southeastern China, the P–T correlation simulated by the INM model was positive (Fig. 8a), which was opposite to observations (Fig. 1a). The INM model simulated a positive correlation over the Arctic and Greenland, as well as over subtropical northern Africa where the observed correlation was weak. The positive correlation over the Antarctic continent had a much larger coverage in the INM model than in observations. In NDJFM, the P–T correlation over equatorial Africa and equatorial South America was opposite that in the observations (Fig. 8b). A positive correlation was simul-

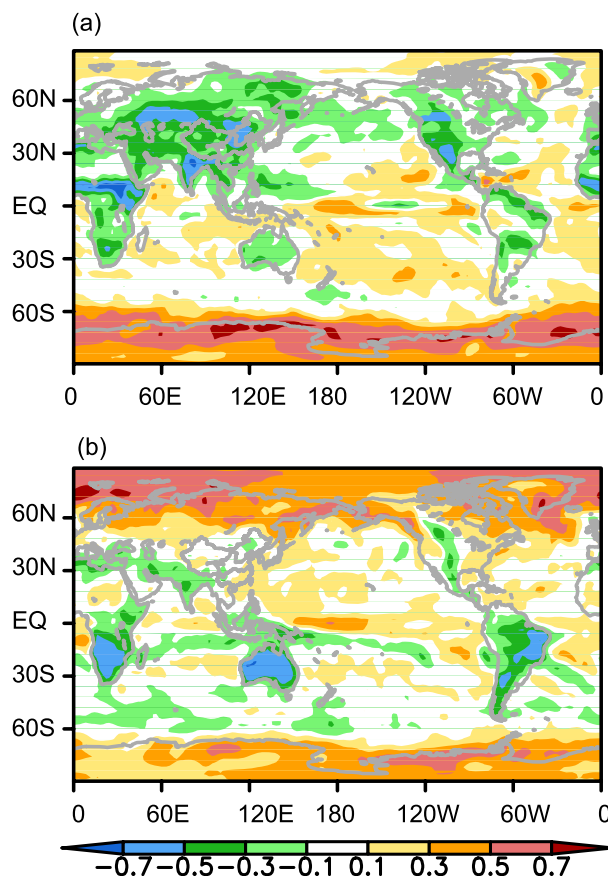


Fig. 9. The same as Fig. 1 except for a single simulation of the MRI model.

ated over subtropical land regions of the Northern Hemisphere, including northern Africa, India, China, and western North America, where the observed correlation was weak or negative (Figs. 8b and 1b). A similar difference was seen over the Arctic region. The positive correlation over the Antarctic region was larger and had a broader coverage compared to observations. In comparison, the INM model performed better over the ocean than over land. Thus, the low pattern correlation of the INM model over the global domain was due to the large differences from observations over the land. This suggests a need for improvement of the land surface component in the INM model.

The distribution of the P–T correlation in the MRI model showed notable differences from observations in several oceanic regions. Specifically, it did not properly represent the positive P–T correlation over the equatorial eastern Pacific Ocean in both MJJAS and NDJFM (Fig. 9). The positive correlation over equatorial Atlantic and Indian Oceans was weaker compared to observations in NDJFM (Fig. 9b). The positive correlation was excessive over the Arctic and Greenland in NDJFM (Fig. 9b) and over the Antarctic coast in both

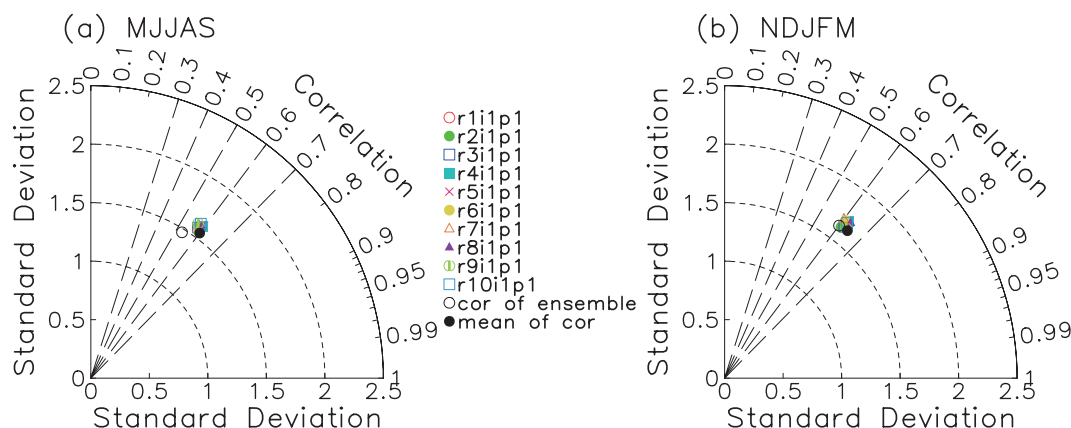


Fig. 10. The same as Fig. 2 except for 10 simulations of CanCM4 model along with the mean of individual correlations and the ensemble mean correlation.

MJJAS and NDJFM (Figs. 9a and b). Over the land regions in the tropics and mid-latitudes, it reproduced the pattern well but with some overestimation in the magnitude of the negative correlation. Overall, the performance of the MRI model was not as good over the ocean as over the land. Thus, a direction for improvement in the MRI model is the oceanic processes and/or the atmosphere–ocean coupling processes, e.g., over the equatorial oceanic regions.

3.3 Spread among model members

In the previous subsections, the evaluation of the model performance was based on a single simulation of individual models. We considered whether the single simulation could represent the other simulations of the same model. To address this issue, we analyzed the correlation for all the members of some subjectively selected models. The spread among the ensemble members versus the difference between model simulations and observations yielded information regarding whether the individual model simulations were representative of other simulations. The analysis also provided useful information about the statistical significance of the difference of the model simulation from the observations (Taylor, 2001).

We calculated the P–T correlation for members of three models. These were MOHC (3 members), NOAA-GFDL (5 members), and CCCMA (10 members). Taylor diagrams were constructed for all three of these models. The results indicate that the spread among the model members were relatively small compared to the difference from the observations. Here, we have shown only the results from the CCCMA model that has the largest number of ensemble simulations (Fig. 10).

Apparently, the pattern correlation and the standard deviation were very close among the members

of the CCCMA model simulations. The spread was much smaller than the distance of the model simulations from the observation reference. This is true for both MJJAS and NDJFM. In comparison, the pattern correlation was somewhat higher in NDJFM than in MJJAS, as was the standard deviation. Figure 10 also shows the points corresponding to the mean of the correlation based on individual members and the correlation based on the ensemble mean. In NDJFM, the two points were quite close, with a difference of ~ 0.04 in the pattern correlation (Fig. 10b). In MJJAS, the two points showed a difference of ~ 0.08 in the pattern correlation (Fig. 10a). The MOHC and GFDL models showed differences between the mean correlation of individual members and the ensemble mean correlation was smaller than those in the CCCMA model (figures not shown).

We examined the distribution of the P–T correlation obtained as the mean correlation of individual members and as the ensemble mean correlation. The distributions were very similar. The P–T correlation based on the ensemble mean of 10 simulations of the CCCMA model is shown in Fig. 11. While the distribution exhibits similarities with observations in the tropics and mid-latitudes, there were some notable differences. In MJJAS, the positive correlation along equatorial Pacific extended too far westward, and the positive correlation along the South Pacific Convergence Zone (SPCZ) was larger and extended too far eastward (Fig. 11a). The positive correlation over equatorial Atlantic Ocean was too weak, compared to observations. The negative correlation over the eastern tropical North Africa was much larger than observations, as was the negative correlation over Australia. In the Arctic and Antarctic regions, the positive correlation was much larger than in observations. In NDJFM, the positive correlation along the SPCZ extended too far

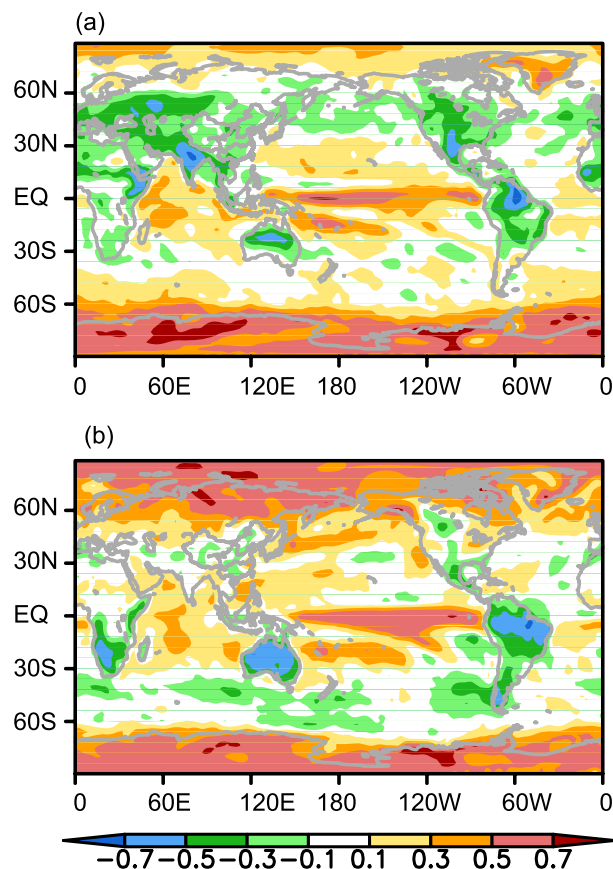


Fig. 11. The same as Fig. 1 except for ensemble mean of the CanCM4 10-member simulations.

eastward (Fig. 11b). The positive correlation over the high-latitudes of the Northern Hemisphere was higher than observations. Very large positive correlation occurred over the Arctic and Antarctic regions.

4. Summary

Precipitation and surface temperature variations may be linked to each other through physical processes that vary from region to region and change from season to season. As such, the P–T relationship can indicate the physical processes in the climate system. For climate models, a proper simulation of the P–T correlation can indicate a model's ability to realistically represent the physical processes and thus the precipitation and surface temperature variations. An improper P–T correlation may degrade the precipitation and surface temperature variations in the models. Thus, it is important to evaluate how well the climate models capture the P–T relationship. In the present study, we compared the P–T correlation between observations and 17 climate models newly available from the IPCC CMIP5 project. The main results are sum-

marized below.

The P–T correlation was mostly positive over the tropical oceans and negative over the mid-latitude lands in both observations and model simulations. The P–T correlation exhibited obvious seasonal change over the land. The negative P–T correlation over the land was large in summer and small in winter. Positive P–T correlation occurred over the high-latitude land regions of the Northern Hemisphere in boreal winter. These results are in general agreement with previous studies.

Based on the pattern correlation, the model performance was better in NDJFM than in MJJAS, except for the mid-latitude lands of the Northern Hemisphere, where the models had the largest pattern correlation with the observations. The model performance was generally better over the land than over the ocean. The seasonal dependence of the model performance was more obvious over the land than over the ocean and more pronounced over the mid- and high-latitudes than over the tropics. All of the models had difficulty capturing the P–T distribution over the mid-latitudes of the Southern Hemisphere in MJJAS.

The spatial variability of the P–T correlation was larger in the models than in observations. The spatial variability of the P–T correlation in the models tended to be larger over the land than over the ocean and increased with the latitude with the smallest variability over the tropical oceans. In the tropics and the high latitudes of the Southern Hemisphere, there was a tendency toward an increase in the spatial variability of the correlation in the models; it was accompanied by an increase in the pattern correlation between model simulations and observations.

Some individual models deviated greatly from the other models in simulating the P–T correlation. Two examples are the INM and MRI models. The INM model had a relatively low pattern correlation, mainly due to its difficulty in capturing the P–T correlation over the land. The MRI model had relatively low pattern correlation due to the improper P–T correlation over the equatorial oceanic regions.

The spread of the P–T correlation among the ensemble members was much smaller compared to the model–observation difference based on evaluation of selected model simulations. The mean of the P–T correlation estimated based on individual members was quite close to the P–T correlation estimated based on ensemble mean.

The evaluation of the P–T correlation provides important information about the performance of the climate models in simulating the co-variability of precipitation and surface temperature. It also gives useful information for potential problems and thus the di-

rection of future improvement of individual models. The specific reasons for discrepancies between model simulations and observations, however, remain elusive at the current stage. The discrepancies over the land may be related to the performance of the land model and those over the Arctic and Antarctic regions may be related to the performance of the sea ice model. The performance may also be related to the capability of the models to simulate the coupled processes, e.g., the ENSO in the tropical Pacific Ocean. Thus, evaluations of other aspects in the models, such as ENSO and land surface energetics, which are expected to be accomplished by other climate scientists, would be beneficial to the understanding of plausible reasons for the model-observation discrepancies in the P–T correlation.

Acknowledgements. This research is jointly supported by the National Key Basic Research Program of China (Grant No. 2009CB421404), the National Natural Science Foundation of China (Grant No. 41175076), the Fundamental Research Funds for the Central Universities (Grant No. 11lgjc10). WU Renguang acknowledges the support of a Direct Grant of the Chinese University of Hong Kong (Grant No. 2021105) and a Hong Kong Research Grants Council Project (CUHK No. 403612). The authors thank Auroral 5000A high-performance computing platform of Sun Yat-Sen University for providing a convenience for downloading model data.

REFERENCES

- Adler, R. F., and Coauthors, 2003: The version 2 global precipitation climatology project (GPCP) monthly precipitation analysis (1979–present). *Journal of Hydrometeorology*, **4**, 1147–1167.
- Idso, S. B., and R. C. Balling Jr., 1992: US temperature/precipitation relationships: implications for future “greenhouse” climates. *Agriculture and Forest Meteorology*, **58**(1–2), 143–147.
- Isaac, G. A., and R. A. Stuart, 1992: Temperature-precipitation relationships for Canadian stations. *J. Climate*, **5**, 822–830.
- Legates, D. R., and C. J. Willmott, 1990: Mean seasonal and spatial variability in global surface air temperature. *Theor. Appl. Climatol.*, **41**, 11–21.
- Madden, R. A., and J. Williams, 1978: The correlation between temperature and precipitation in the United States and Europe. *Mon. Wea. Rev.*, **106**, 142–147.
- Power, S., F. Tseitkin, V. Mehta, B. Lavery B, S. Torok, and N. Holbrook, 1999: Decadal climate variability in Australia during the twentieth century. *Int. J. Climatol.*, **19**, 169–184.
- Rebetez, M., 1996: Seasonal relationship between temperature, precipitation and snow cover in a mountainous region. *Theor. Appl. Climatol.*, **54**(3–4), 99–106.
- Rusticucci, M., and O. Penalba, 2000: Interdecadal changes in the precipitation seasonal cycle over southern South America and their relationship with surface temperature. *Climate Research*, **16**, 1–15.
- Smith, T. M., R. W. Reynolds, T. C. Peterson, and J. Lawrimore, 2008: Improvements to NOAA’s historical merged land-ocean surface temperature analysis (1880–2006). *J. Climate*, **21**, 2283–2296.
- Taylor, K. E., 2001: Summarizing multiple aspects of model performance in single diagram. *J. Geophys. Res.*, **106**, D7, 7183–7192.
- Taylor, K. E., R. J. Stouffer, and G. A. Meehl, 2012: An overview of CMIP5 and the experiment design. *Bull. Amer. Meteor. Soc.*, **93**, 485–498, doi: 10.1175/BAMS-D-11-00094.1.
- Tout, D. G., 1987: Precipitation-temperature relationship in England and Wales summers. *Int. J. Climatol.*, **7**(2), 181–184.
- Trenberth, K. E., and D. J. Shea, 2005: Relationships between precipitation and surface temperature. *Geophys. Res. Lett.*, **32**, L14703, doi: 10.1029/2005GL022760.
- Vose, R. S., R. L. Schmoyer, P. M. Steuer, T. C. Peterson, R. Heim, T. R. Karl, and J. K. Eischeid, 1992: *The Global Historical Climatology Network: long-term monthly temperature, precipitation, sea level pressure and station pressure data*. ND-P 041, Carbon Dioxide Information Analysis Center, Oak Ridge National Laboratory, Tennessee, USA, 26pp.
- Wang, J.-J., R. F. Adler, and G. Gu, 2008: Tropical rainfall-surface temperature relations using tropical rainfall measuring mission precipitation data. *J. Geophys. Res.*, **113**, D18115, doi: 10.1029/2007JD009540.
- Wu, B., T. Zhou, and T. Li, 2009: Contrast of rainfall-SST relationships in the western North Pacific between the ENSO-developing and ENSO-decaying summers. *J. Climate*, **22**, 4398–4405.
- Wu, R., and B. P. Kirtman, 2007: Regimes of local air-sea interactions and implications for performance of forced simulations. *Climate Dyn.*, **29**, 393–410.
- Wu, R., and J. L. Kinter III, 2010: Atmosphere-ocean relationship in the midlatitude North Pacific: Seasonal dependence and east-west contrast. *J. Geophys. Res.*, **115**, D06101, doi: 10.1029/2009JD012579.
- Wu, R., B. P. Kirtman, and K. Pegion, 2006: Local air-sea relationship in observations and model simulations. *J. Climate*, **19**, 4914–4932.
- Zhao, W., and M. A. K. Khalil, 1993: The relationship between precipitation and temperature over the contiguous United States. *J. Climate*, **6**, 1232–1236.